Korean J. Chem. Eng., **27**(1), 49-54 (2010)
DOI: 10.2478/s11814-009-0290-8

NO oxidation over supported cobalt oxide catalysts

Dae Su Kim*, Yun Ha Kim*, Jae Eui Yie, and Eun Duck Park*,†**

*Division of Energy Systems Research and Division of Chemical Engineering and Materials Engineering,
**Division of Applied Biotechnology,
Ajou University, San 5 Wonchun-dong, Yeongtong-gu, Suwon 443-749, Korea
(*Received 14 April 2009 • accepted 23 May 2009*)

Abstract−NO oxidation was conducted over cobalt oxides supported on various supports such as SiO_2, ZrO_2, TiO_2, and CeO_2. The N_2 physisorption, an inductively coupled plasma-atomic emission spectroscopy (ICP-AES), X-ray diffraction (XRD), NO chemisorptions, the temperature-programmed desorption (TPD) with a mass spectroscopy after NO or CO chemisorptions were conducted to characterize catalysts. Among tested catalysts, Co_3O_4 supported on ceria with a high surface area showed the highest catalytic activity. This catalyst showed superior catalytic activity to unsupported Co_3O_4 with a high surface area and 1 wt% Pt/γ-Al_2O_3. For ceria-supported Co_3O_4, the catalytic activity, the NO uptake at 298 K and the dispersion of Co_3O_4 increased with increasing the surface area of CeO_2. The active participation of the lattice oxygen in NO oxidation could not be observed. On the other hand, the lattice oxygen participated in the CO oxidation over the same catalyst. The deactivation was observed over Co_3O_4/CeO_2 and 1 wt% Pt/γ-Al_2O_3 in the presence of SO_2 in a feed. 1 wt% Pt/γ-Al_2O_3 was deactivated by SO_2 more rapidly compared with Co_3O_4/CeO_2.

Key words: NO Oxidation, Co_3O_4, Supports, CeO_2, TPD

INTRODUCTION

Nitrogen oxides (NO_x), emitted from stationary and mobile sources, have been reported to cause several environmental problems such as acid rain, photochemical smog, ozone layer destruction, and green house effect, etc. [1]. Therefore, the regulation against NO_x emission has recently been strengthened with increasing the concern for environmental issues. To meet this requirement, various methods for NO_x control have been examined, such as selective catalytic reduction (SCR), NO_x storage and reduction (NSR) and selective NO_x recirculation (SNR) [1-5]. Among them, the SCR can be regarded as one of representative ways to decrease NO_x concentration in the flue gas. This SCR reaction rate has been reported to be directly dependent on the fraction of NO_2 in NO_x [6-10]. The enhancement in the de-NO_x rate can be noticeable especially at low temperatures such as 200-300 °C when equimolar amounts of NO and NO_2 are present in a feed (fast SCR process). This fast SCR process (1) can give us a way to decrease the reactor size compared with the standard SCR process (2), especially at low temperatures.

$$2NH_3+NO+NO_2 \rightarrow 2N_2+3H_2O \quad (1)$$

$$2NH_3+2NO+1/2O_2 \rightarrow 2N_2+3H_2O \quad (2)$$

Besides NH_3-SCR, the presence of NO_2 in a feed has been frequently reported to be beneficial for the conversion of NO into N_2 for the SCR of NO with hydrocarbons [11-18].

In the lean burning natural gas or diesel engine, NO_x is mainly composed of NO. Therefore, the oxidation of NO into NO_2 can be an important reaction for NO_x control. Until now, several catalyst systems have been examined for NO oxidation. They can be grouped into the noble metals [19-33] and the transition metal oxides [34-46] catalysts. H. Ohtsuka applied noble metal-loaded sulfated zirconia to the SCR with methane and found that Ru, Ir and Pt catalysts showed high activity for NO oxidation [19]. Among noble metal catalysts, supported Pt-based catalysts have been intensively examined [20-32]. The NO oxidation activity has been reported to increase with increasing the particle size of Pt [20]. Based on high throughput experiments, Schmitz et al. reported that the relative order of importance of the factors evaluated was support>pretreatment>loading>calcinations atmosphere>calcinations temperature>precursor salt [26]. Besides of its high price, the development of a catalyst system based on the transition metal oxides is required to substitute Pt-based catalysts because this Pt-based catalyst has been reported to be deactivated by several causes. Decreasing NO oxidation activity was observed with concomitant phase transformation from Pt to PtO_x [28,29]. The presence of SO_2 and H_2O was also reported to decrease the catalytic activity via formation of sulfate on the support [29-31] and decrease in Pt surface area [32], respectively. As transition metal oxides, various catalyst systems have been examined such as CuO/SiO_2-Al_2O_3(-TiO_2, -ZrO_2) [34], CuO/NiO/alumina [35], CuO/NiO/titania [35], Ag/Al_2O_3 [36], Ga-ZSM-5 [37], In-ZSM-5 [37], Fe-MFI [38,39], Fe-FER [38], Co/Al_2O_3 [40], Co-H-MFI [41], Co-H-FER [42], Co/TiO_2 [43], Co/ZrO_2 [43], Co/$K_xTi_2O_5$ [44,45] and Co_3O_4 [46]. Until now, Co-based catalyst systems have been frequently reported to have promising catalytic activity for NO oxidation. However, few comparison works among supported cobalt oxides have been conducted systematically. Yung et al. compared the NO oxidation activity between Co/TiO_2 and Co/ZrO_2 and reported that 10% Co/ZrO_2 prepared by an incipient-wetness impregnation technique was the most active [43].

In this study, cobalt oxides catalysts prepared with different supports and cobalt contents were compared for the NO oxidation.

†To whom correspondence should be addressed.
E-mail: edpark@ajou.ac.kr

EXPERIMENTAL

1. Preparation of Catalysts

All the catalysts were prepared with a wet impregnation method from an aqueous solution of cobalt acetate ($Co(CH_3COO)_2 \cdot 4H_2O$, Junsei Chem.). For example, the Co_3O_4/SiO_2 containing 10 wt% Co was prepared as follows. An aqueous solution of cobalt acetate was prepared by dissolving 2.34 g of $Co(CH_3COO)_2 \cdot 4H_2O$ in 50 ml of deionized water. 5.0 g of SiO_2 was put into the solution and mixed with 60 rpm in a rotary evaporator at an atmospheric pressure at 333 K for 6 h. The excess water was evaporated at 333 K in a vacuum condition and the impregnated sample was recovered and dried in an oven at 393 K for 12 h. The dried sample was calcined in air at 573 K before a reaction.

Metal oxides such as TiO_2 (Degussa, P-25, S_{BET}=51.3 m^2/g), CeO_2 (Rhodia, denoted as CeO_2 (H), S_{BET}=300 m^2/g), and SiO_2 (Aldrich, S_{BET}=348.7 m^2/g) were purchased and utilized as a support. Additionally, CeO_2(M) and ZrO_2 were prepared with a precipitation method from $Ce(NO_3)_3 \cdot H_2O$ (Kanto Chemical) and $ZrOCl_2 \cdot 8H_2O$ (Junsei Chem.), respectively. 1 M NaOH solution and 1 M NH_4OH solution were utilized as a precipitation agent for each sample and the precipitant was filtered, dried at 393 K and calcined in air at 773 K before use as a support. The BET surface area was determined to be 74 m^2/g and 94 m^2/g for CeO_2 (M) and ZrO_2, respectively.

The cobalt oxide (Co_3O_4) was prepared by a precipitation method. The pH of an aqueous solution of $Co(NO_3)_2$ was increased to 8 by an addition of 1 M NaOH solution. The slurry was aged for 1 h at 353 K, filtered, and washed with deionized water several times to remove sodium ion. The cake was then dried at 373 K overnight. Cobalt oxide was finally calcined in air at 573 K before a reaction.

1 wt% Pt/g-Al_2O_3 was purchased from Aldrich and utilized as a reference catalyst. All the catalysts were calcined at 573 K in air for 1 h before a reaction. Its BET surface area was determined to be 94 m^2/g.

2. Characterization of Catalysts

The BET surface area was calculated from N_2 adsorption data that were obtained by using the Autosorb-1 apparatus (Quantachrome) at liquid N_2 temperature. Before the measurement, the sample was degassed in vacuum for 4 h at 473 K.

Chemical composition of the prepared samples was analyzed by inductively coupled plasma-atomic emission spectroscopy (ICP-AES, JY-70Plus, Jobin-Yvon); the results are listed in Table 1 and 2.

Bulk crystalline structures of catalysts were determined with an X-ray diffraction (XRD) technique. XRD patterns were recorded on a Rigaku D/MAC-III using Cu Kα radiation (λ=0.15406 nm), operated at 40 kV and 100 mA (4.0 kW). The crystalline size of CeO_2 and Co_3O_4 was calculated by applying the Scherrer line broadening equation as follows [47].

$$L = \frac{0.9\lambda_{K_{\alpha 1}}}{B_{(2\theta)}\cos\theta_{max}}$$

where L denotes the average particle size, the value 0.9 is chosen when $B_{(2\theta)}$ is the full width at half maximum (FWHM) of the peak broadening in radians, $\lambda_{K_{\alpha 1}}$ is the wavelength of X-ray radiation (0.15406 nm), and θ_{max} is the angular position at the (111) peak maximum of CeO_2 and at the (311) peak maximum of Co_3O_4, respectively.

NO uptake measurements were performed in an AutoChem 2,910 unit (Micromeritics) equipped with a thermal conductivity detector (TCD) to measure NO consumption and an on-line mass spectrometer (QMS 200, Pfeiffer Vacuum) to detect any organic or inorganic species in the effluent stream during NO uptake experiment. Quartz U-tube reactors were loaded with 0.1 g of sample. In the case of 1 wt% Pt/γ-Al_2O_3, 0.5 g of sample was used to obtain more reliable data because much smaller amounts of NO appeared to be chemisorbed on this catalyst compared with those of supported cobalt oxides catalysts. All the catalysts were pretreated by calcinations in 20 vol% O_2 in N_2 at 573 K for 1 h, then cooled to room temperature. The NO uptake measurement was carried out at 298 K in 30 cm^3/min of He stream through a pulsed-chemisorption technique, in which 50 μl pulses of NO were used, after any residual oxygen in a line was removed by flowing He at 298 K for 1 h.

The temperature programmed desorption (TPD) of NO was carried out after NO chemisorption at 298 K in an AutoChem 2,910 unit (Micromeritics) and an on-line mass spectrometer (QMS 200, Pfeiffer Vacuum) to analyze the desorbed species in the effluent stream during TPD experiment. After NO chemisorption at 298 K, the TPD was performed using 30 cm^3/min of He from 313 K to 573 K at a heating rate of 10 K/min monitoring the mass signals after any residual species in a line were removed by flowing He at 313 K for 1 h.

The CO chemisorption was also conducted for 1 wt% Pt/γ-Al_2O_3 in the same way as described in the NO chemisorption, except that 0.2 g of sample was used after reduction in H_2 at 573 K for 1 h and that CO was used instead of NO after any residual hydrogen in a line was removed by flowing He at 300 K for 1 h.

The temperature programmed desorption (TPD) of CO was carried out for Co_3O_4 after CO chemisorption at 298 K in the same way as mentioned in the NO-TPD, except that 0.1 g of Co_3O_4 calcined in 20 vol% O_2 in N_2 at 573 K for 1 h was utilized.

Table 1. The physicochemical properties of cobalt oxides supported on various supports and unsupported Co_3O_4

Catalysts	Co content (wt%)	Surface area (m^2/g)	NO uptake at 298 K ($\mu mol_{NO}/g_{cat.}$)
Co_3O_4/CeO_2(H)	9.5	230	504
Co_3O_4/CeO_2(M)	9.6	66	47
Co_3O_4/ZrO_2	9.5	86	17
Co_3O_4/TiO_2	9.1	57	9
CoO_x/SiO_2	8.1	272	48
Co_3O_4	72.6	65	146

Table 2. The physicochemical properties of Co_3O_4/CeO_2(H) containing different amounts of Co

Co content (wt%)	Surface area (m^2/g)	NO uptake at 298 K ($\mu mol/g_{cat.}$)
4.1	256	369
6.2	253	499
7.8	252	513
9.5	230	504
12.2	230	388
16.1	228	366

3. Activity Test

The catalytic activity was measured in a small fixed bed reactor of 8-mm i.d. with catalysts that had been retained between 45 and 80 mesh sieves. Reactant gases were fed to the reactor by means of electronic mass flow controller (MKS). The reactant gas typically consisted of 500 ppm NO and 5 vol% O_2 in N_2. All the lines were heated above 423 K to prevent any gas from condensation. For a typical screening experiment, 0.15 g of catalyst was contacted with the reactant gas with a total flow rate of 200 ml/min. The NO_x concentration in the inlet and outlet gas was analyzed by means of a NO/NO_2 combustion gas analyzer (Euroton). From the concentration of the gases at steady state, NO conversion can be calculated according to the following formula:

$$\text{NO Conversion } (\%) = \frac{[NO]_{in} - [NO]_{out}}{[NO]_{in}} \times 100$$

The subscripts in and out indicated the inlet concentration and outlet concentration at steady state, respectively.

RESULTS AND DISCUSSION

The cobalt contents and the surface areas for all prepared catalysts are presented in Table 1 and 2. The effect of kinds of support on NO oxidation in the dry condition was examined over cobalt oxides supported on different supports as shown in Fig. 1. Unsupported Co_3O_4 and 1 wt% $Pt/\gamma\text{-}Al_2O_3$ were also tested at the same reaction condition. The catalytic activity for NO oxidation decreased in the following order: $Co_3O_4/CeO_2(H)$~1 wt% $Pt/\gamma\text{-}Al_2O_3$>>Co_3O_4> CoO_x/SiO_2>$Co_3O_4/CeO_2(M)$>Co_3O_4/ZrO_2>Co_3O_4/TiO_2. The most active catalyst, $Co_3O_4/CeO_2(H)$, has a comparable catalytic activity for this reaction over all reaction temperatures with a well-known noble metal catalyst, $Pt/\gamma\text{-}Al_2O_3$. The amount of chemisorbed CO on 1 wt% $Pt/\gamma\text{-}Al_2O_3$ was determined to be 26.4 $\mu mol_{CO}/g_{cat.}$, which could be interpreted that the Pt dispersion was 51% based on the assumption that CO could be chemisorbed on surface Pt atom linearly. This $Co_3O_4/CeO_2(H)$ exhibited superior catalytic activity to Co_3O_4 even at the same contact time. Irfan et al. [46] reported that unsupported Co_3O_4 was the most active catalysts for NO oxidation and also found that its catalytic activity as well as its surface area decreased with increasing calcination temperature. In this work, we could prepare Co_3O_4 with a higher surface area than that reported by Irfan et al. [46]. Therefore, it can be concluded that the catalytic activity of cobalt oxides catalysts can be increased further by choosing the proper supports. While comparing the catalytic activity among Co_3O_4 supported on ceria with different surface areas, we have found that the catalytic activity for NO oxidation is strongly dependent on the surface area of CeO_2. The catalytic activity for NO oxidation increased with increasing the surface area of ceria.

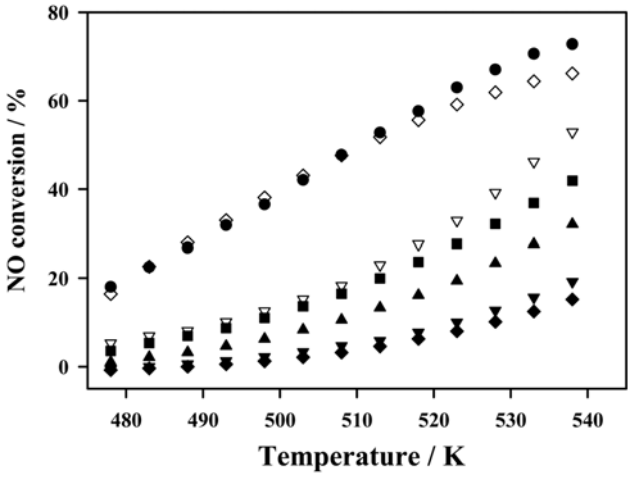

Fig. 1. NO conversion at different reaction temperatures over cobalt oxide catalysts supported on various supports such as (●) $CeO_2(H)$, (■) SiO_2, (▲) $CeO_2(M)$, (▼) ZrO_2, and (◆) TiO_2. The cobalt content for each catalyst is listed in Table 1. Co_3O_4 (▽) and 1 wt% Pt/Al_2O_3 (◇) are also included. Reactants: 500 ppm NO, 5% O_2 in N_2. 0.15 g of catalyst was contacted with the reactant gas with a total flow rate of 200 ml/min.

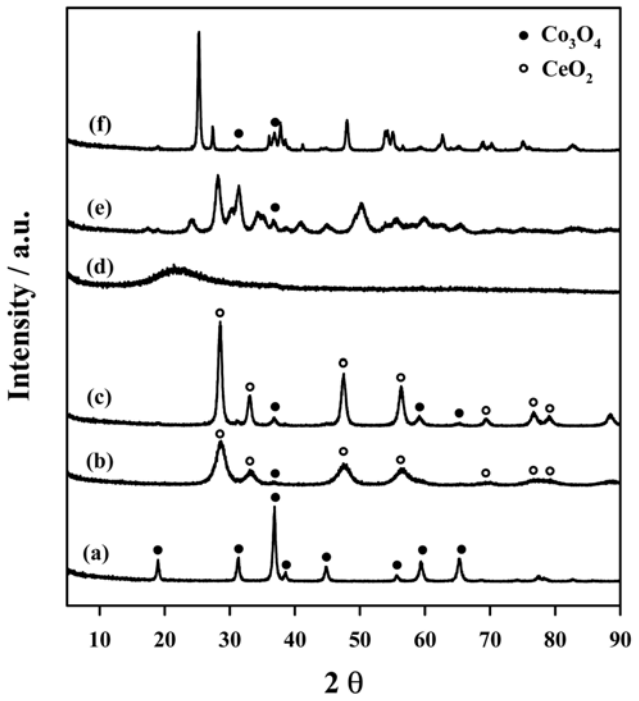

Fig. 2. X-ray diffraction patterns of Co_3O_4 (a) and cobalt oxides supported on various supports such as $CeO_2(H)$ (b), CeO_2 (M) (c), SiO_2 (d), ZrO_2 (e), and TiO_2 (f). The cobalt content for each catalyst was listed in Table 1. All these catalysts were calcined in air at 573 K before an experiment.

The NO uptake was obtained at 298 K for unsupported Co_3O_4 and cobalt oxides supported on various supports and listed in Table 1. The specific NO uptake decreased in the following order: $Co_3O_4/CeO_2(H)$>>Co_3O_4>CoO_x/SiO_2~$Co_3O_4/CeO_2(M)$>Co_3O_4/ZrO_2>Co_3O_4/TiO_2. The $Co_3O_4/CeO_2(H)$ shows the largest NO uptake, which is larger than any other supported catalysts by at least 10 times. No detectable NO uptake can be obtained for $CeO_2(H)$. Therefore, the NO chemisorptions can be regarded to be due to the presence of Co_3O_4 in the catalyst. Because the order among different supported cobalt oxides catalysts for the specific NO uptake is same with that of the catalytic activity for NO oxidation, it can be said that the catalytic activity increases with the NO uptake among examined supported cobalt oxides catalysts. In the case of 1 wt% $Pt/\gamma\text{-}Al_2O_3$, the NO uptake at 298 K was determined to be 1.6 $\mu mol_{NO}/g_{cat.}$, which

is far less than those of supported cobalt oxides catalysts.

X-ray diffraction patterns were obtained for all tested samples as shown in Fig. 2. Except for CoO_x/SiO_2, Co_3O_4 was the only observable crystalline structure for cobalt species. No noticeable XRD peak corresponding to Co_3O_4 can be found for CoO_x/SiO_2. Based on the Scherrer line broadening equation, the crystalline size of Co_3O_4 for unsupported Co_3O_4 was determined to be 19.3 nm. In the case of Co_3O_4 supported on ceria with a different surface area, the XRD peak corresponding to CeO_2 and Co_3O_4 was strengthened with decreasing its surface area. The crystalline size of ceria for Co_3O_4/CeO_2(H) and Co_3O_4/CeO_2(M) was determined to be 4.5 nm and 12.0 nm, respectively. The crystalline size of ceria increased with decreasing its surface area. Although the presence of crystalline phase of Co_3O_4 can be confirmed in Co_3O_4/CeO_2(H), the crystalline size of Co_3O_4 cannot be calculated because of its broad and weak peak intensity. On the other hand, the crystalline size of Co_3O_4 in Co_3O_4/CeO_2(M) was determined to be 10.2 nm. The crystalline size of Co_3O_4 decreased with increasing the surface area of CeO_2.

The effect of cobalt content on the BET surface area and the specific NO uptake was investigated over cobalt oxides supported on the high-surface area CeO_2 as shown in Table 2. The BET surface area decreased with increasing cobalt contents. The specific NO uptake increased, showed the maximum value when the cobalt content was 7.8 wt%, and then decreased with further increasing the cobalt content. The effect of cobalt content on the catalytic activity for NO oxidation was also examined over cobalt oxides supported on the high-surface area CeO_2 as shown in Fig. 3. At the same contact time, the NO conversion increased, showed the maximum value, and then decreased with increasing the cobalt content. This catalytic activity for NO oxidation with increasing the Co content is in line with the specific NO uptake at 298 K.

Fig. 4 shows the XRD patterns for Co_3O_4/CeO_2(H) containing different amounts of Co. For Co_3O_4/CeO_2(H) with the cobalt content of 7.8 wt% and less, no representative XRD peaks corresponding cobalt species can be found. Only when the cobalt content was 9.64 wt% and above it, the XRD peaks representing Co_3O_4 appeared

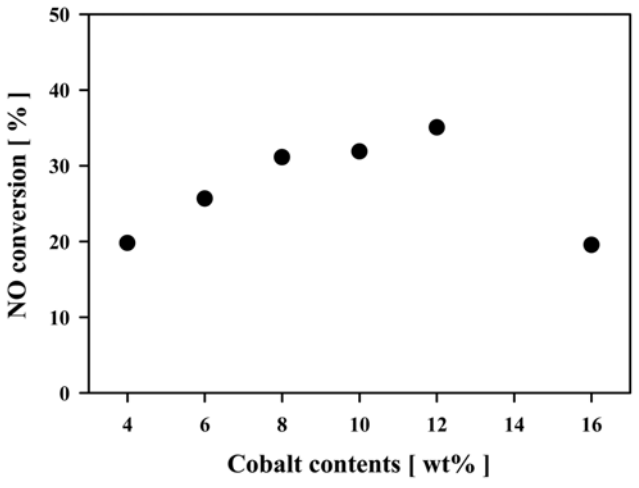

Fig. 3. NO conversion at 493 K over Co_3O_4/CeO_2(H) containing different cobalt contents. Reactants: 500 ppm NO, 5% O_2 in N_2. 0.15 g of catalyst was contacted with the reactant gas with a total flow rate of 200 ml/min.

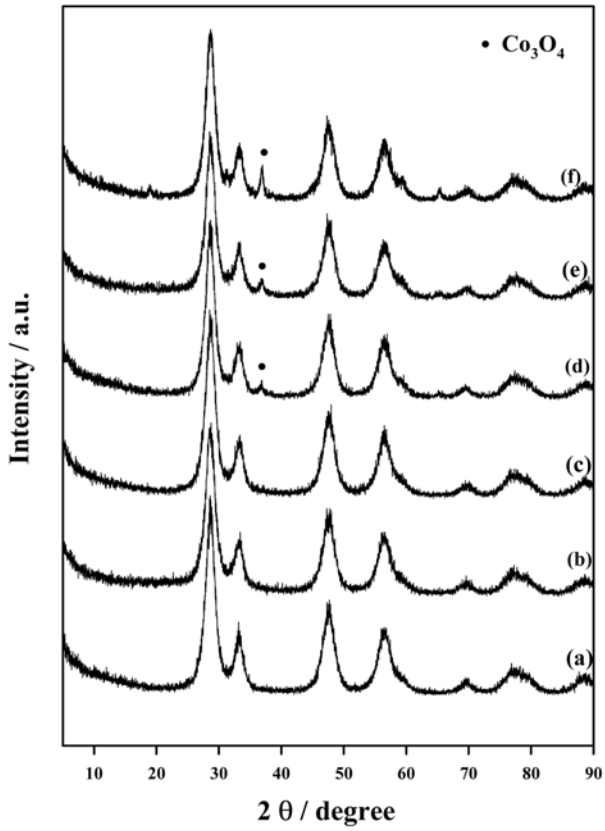

Fig. 4. X-ray diffraction patterns of Co_3O_4/CeO_2(H) containing different amounts of cobalt such as (a) 4.1, (b) 6.2, (c) 7.8, (d) 9.6, (e) 12.2, and (f) 16.1 wt%. All these catalysts were calcined in air at 573 K before an experiment.

and these peaks were strengthened with increasing Co content. This implies that the crystalline size of Co_3O_4 increased with increasing the cobalt content. Based on the Scherrer line broadening equation, the crystalline size of Co_3O_4 for Co_3O_4/CeO_2(H) containing 12.2 wt% Co was determined to be 7.5 nm, which is much smaller than that of unsupported Co_3O_4. It can be assumed that the crystalline size of Co_3O_4 is smaller than 7.5 nm for Co_3O_4/CeO_2(H) containing less than 12.2 wt% Co. The increasing crystalline size of Co_3O_4 for Co_3O_4/CeO_2(H) with increasing the Co content can be confirmed by the fact that the crystalline size of Co_3O_4 for Co_3O_4/CeO_2(H) containing 16.1 wt% Co was determined to be 11.0 nm, which is larger than that of Co_3O_4 for Co_3O_4/CeO_2(H) containing 12.2 wt% Co.

Temperature programmed desorption (TPD) after NO chemisorptions at 298 K was conducted to find out whether the lattice oxygen can take part in NO oxidation or not over Co_3O_4/CeO_2(H) and unsupported Co_3O_4 as shown in Fig. 5. Interestingly, NO_2 was not detected during TPD till 573 K, which supports the fact that the lattice oxygen does not contribute on NO oxidation. Only NO was desorbed at different temperature, which implies that there are different adsorption sites for NO chemisorptions. For comparison, temperature programmed desorption (TPD) after CO chemisorptions at 298 K was conducted to find out whether the lattice oxygen can take part in CO oxidation or not over unsupported Co_3O_4 as shown in Fig. 6. CO was desorbed and the evolution of CO_2 was observed at different temperatures. This can be strong evidence that the lattice

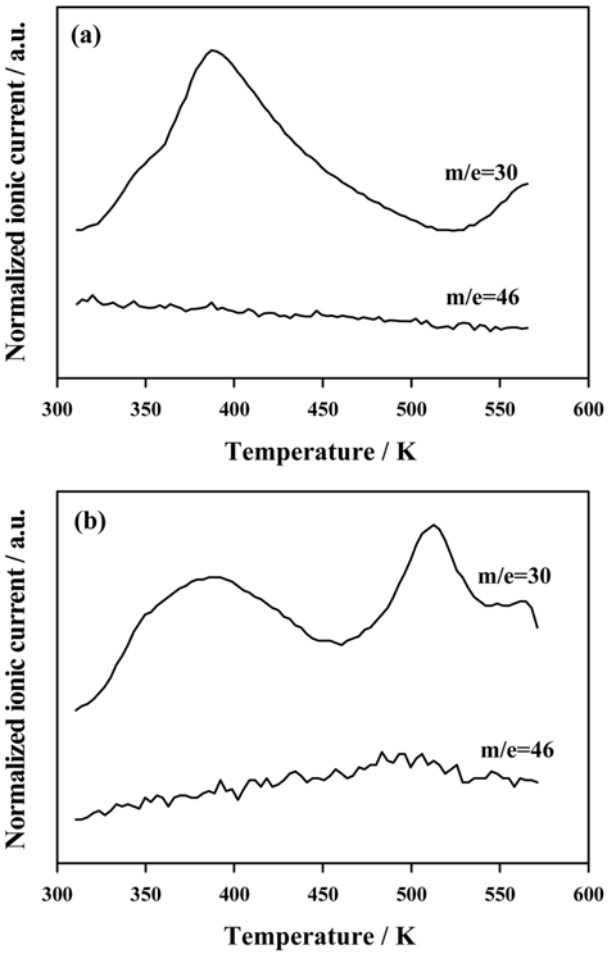

Fig. 5. Temperature programmed desorption (TPD) patterns of NO adsorbed on (a) Co_3O_4/CeO_2(H) containing 9.6 wt% Co and (b) Co_3O_4.

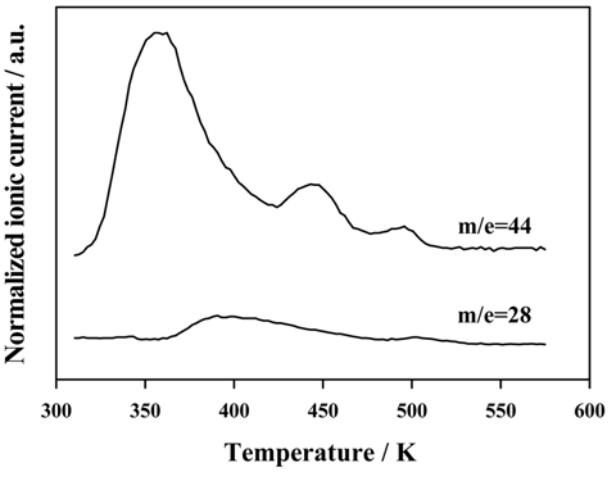

Fig. 6. Temperature programmed desorption (TPD) patterns of CO adsorbed on Co_3O_4.

oxygen can participate in CO oxidation. Based on these results, NO oxidation occurs via surface oxygen-mediated mechanism not through lattice oxygen-mediated one.

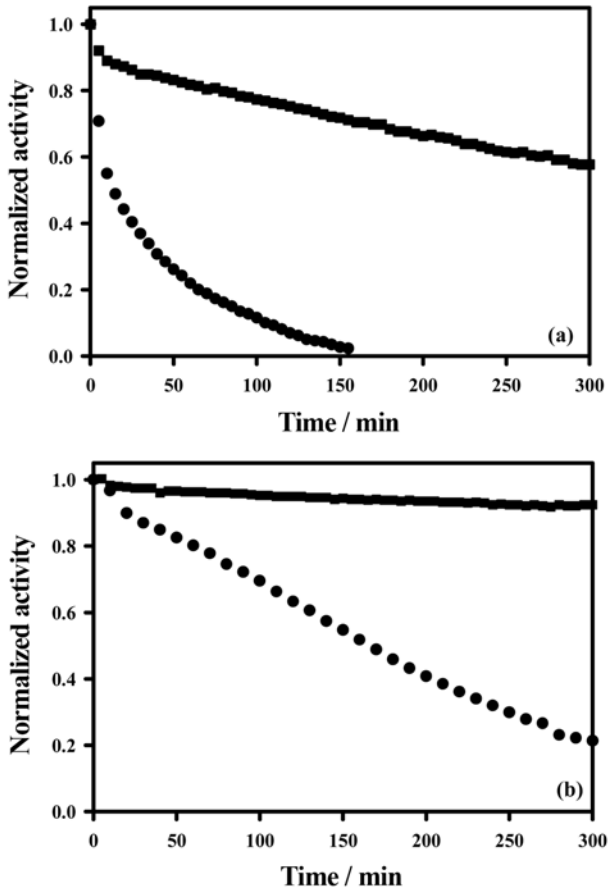

Fig. 7. The normalized activity at 543 K over 1 wt% Pt/Al_2O_3 (a) and Co_3O_4/CeO_2(H) containing 9.6 wt% Co (b) in the presence of SO_2 in a different ppm level such as (●) 100 ppm and (■) 10 ppm. This normalized activity was calculated by determining the NO conversion in the presence of SO_2 with the NO conversion in the absence of SO_2. Reactants: 500 ppm NO, x ppm SO_2, 5% O_2 in N_2. 0.15 g of catalyst was contacted with the reactant gas with a total flow rate of 200 ml/min.

The catalytic stability in the presence of SO_2 in a feed was investigated over 1 wt% Pt/γ-Al_2O_3 and Co_3O_4/CeO_2(H) as shown in Fig. 7. Both catalysts were deactivated in the presence of SO_2 in a feed. Co_3O_4/CeO_2(H) was more resistant to SO_2 poisoning compared with 1 wt% Pt/γ-Al_2O_3. The deactivation rate increased with increasing SO_2 concentration in a feed. This deactivation due to SO_2 in a feed was confirmed to be irreversible based on the experimental result that the decreased NO conversion did not increase but maintained after interrupting SO_2 supply in a feed. The cause of the deactivation phenomenon over Co_3O_4/CeO_2(H) in the presence of SO_2 in a feed can be explained by the fact that the NO uptake decreased significantly after exposure to SO_2 in a feed. The active site for NO chemisorptions might be blocked by the adsorbed SO_2 species, and thus the reaction rate decreases steadily in the presence of SO_2 in a feed.

CONCLUSIONS

Cobalt oxides supported on ceria with a high surface area showed

the highest catalytic activity for NO oxidation among cobalt oxides supported on SiO_2, ZrO_2, TiO_2, and CeO_2. This catalyst showed comparable catalytic activity with 1 wt% Pt/γ-Al_2O_3. It also showed superior catalytic activity to unsupported Co_3O_4 with a high surface area. For ceria-supported Co_3O_4, the catalytic activity, the NO uptake at 298 K and the dispersion of Co_3O_4 increased with increasing the surface area of CeO_2. The catalytic activity for NO oxidation appears to be closely related with the NO uptake at 298 K for tested supported cobalt oxides catalysts. The active participation of the lattice oxygen in NO oxidation cannot be observed. On the other hand, the lattice oxygen participated in the CO oxidation over the same catalyst. Irreversible deactivation was observed over Co_3O_4/CeO_2 and 1 wt% Pt/γ-Al_2O_3 in the presence of SO_2 in a feed. 1 wt% Pt/γ-Al_2O_3 was deactivated by SO_2 more rapidly compared with Co_3O_4/CeO_2.

ACKNOWLEDGMENT

This work was supported by the Korea Research Foundation Grant funded by the Korean Government (MEST) (KRF-2007-412-J04001).

REFERENCES

1. A. Fritz and V. Pitchon, *Appl. Catal. B: Environ*., **13**, 1 (1997).
2. Y. U. Murzin, *Acc. Chem. Res*., **39**, 273 (2006).
3. B. A. A. L. van Setten, M. Makkee and J. A. Moulijn, *Catal. Rev. Sci*., **43**, 489 (2001).
4. M. A. Gómez-García, V. Pitchon and A. Kiennemann, *Envir. Inter*., **31**, 445 (2005).
5. Z. Liu and S. I. Woo, *Catal. Rev. Sci*., **48**, 43 (2006).
6. M. Koebel, G. Madia and M. Elsener, *Catal. Today*, **73**, 239 (2002).
7. A. Wokaun, *Ind. Eng. Chem. Res*., **41**, 4008 (2002).
8. G. Madia, M. Kebel, M. Elsener and A. Wokaun, *Ind. Eng. Chem. Res*., **41**, 3512 (2002).
9. M. Koebel, M. Elsener and M. Kleemann, *Catal. Today*, **59**, 335 (2000).
10. M. Kang, D. J. Kim, E. D. Park, J. M. Kim, J. E. Yie, S. H. Kim, L. Hope-Weeks and E. M. Eyring, *Appl. Catal. B: Environ*., **68**, 21 (2006).
11. M. D. Amiridis, T. Zhang and R. J. Farrauto, *Appl. Catal. B: Environ*., **10**, 203 (1996).
12. M. J. Castagnola, M. K. Neylon and C. L. Marshall, *Catal. Today*, **96**, 61 (2004).
13. J. R. Regalbuto, T. Zheng and J. T. Miller, *Catal. Today*, **54**, 495 (1999).
14. F. C. Meunier and J. R. H. Ross, *Appl. Catal. B: Environ*., **24**, 23 (2000).
15. J. O. Petunchi and W. K. Hall, *Appl. Catal. B: Environ*., **2**, L17 (1993).
16. A. Yu. Stakheev, C. W. Lee, S. J. Park and P. J. Chong, *Catal. Lett*., **38**, 271 (1996).
17. A. Yu. Stakheev, C. W. Lee, S. J. Park and P. J. Chong, *Appl. Catal. B: Environ*., **9**, 65 (1996).
18. P. W. Park, C. S. Ragle, C. L. Boyer, M. L. Balmer, M. Engelhard and D. McCready, *J. Catal.*, **210**, 97 (2002).
19. H. Ohtsuka, *Appl. Catal. B: Environ*., **33**, 325 (2001).
20. F. Jayat, C. Lembacher, U. Schubert and J. A. Martens, *Appl. Catal. B: Envirion*., **21**, 221 (1999).
21. L. Olsson, B. Westerberg, H. Persson, E. Fridell, M. Skoglundh and B. Andersson, *J. Phys. Chem. B*, **103**, 10433 (1999).
22. J. Després, M. Elsener, M. Koebel, O. Kröcher, B. Schnyder and A. Wokaun, *Appl. Catal. B: Environ*., **50**, 73 (2004).
23. J. Dawody, M. Skoglundh and E. Fridell, *J. Mol. Catal. A*, **209**, 215 (2004).
24. M. Crocoll, S. Kureti and W. Wisweiler, *J. Catal*., **229**, 480 (2005).
25. Y. Ji, T. J. Toops, U. M. Graham, G. Jacobs and M. Crocker, *Catal. Lett*., **110**, 29 (2006).
26. P. J. Schmitz, R. J. Kudla, A. R. Drews, A. E. Chen, C. K. Lowe-Ma, R. W. McCave, W. F. Schneider and C. T. Goralski Jr., *Appl. Catal. B: Environ*., **67**, 246 (2006).
27. M. F. Irfan, J. H. Goo, S. D. Kim and S. C. Hong, *Chemosphere*, **66**, 54 (2007).
28. L. Olsson and E. Fridell, *J. Catal*., **210**, 340 (2002).
29. R. Marques, P. Darcy, P. D. Costa, H. Mellottée, J. M. Trichard and G. Djéra-Mariadassou, *J. Mol. Catal. A*, **221**, 127 (2004).
30. E. Xue, K. Seshan and J. R. H. Ross, *Appl. Catal. B: Environ*., **11**, 65 (1996).
31. E. Xue, K. Seshan and J. G. van Ommen, *Appl. Catal. B: Environ.*, **2**, 183 (1993).
32. S. S. Mulla, N. Chen, L. Cumaranatunge, G. E. Blau, D. Y. Zemlyanov, W. N. Delgass, W. W. Epling and F. H. Ribeiro, *J. Catal.*, **241**, 389 (2006).
33. L. Li, L. Qu, J. Cheng, J. Li and Z. Hao, *Appl. Catal. B: Environ.*, **88**, 224 (2009).
34. S. Bennici and A. Gervasini, *Appl. Catal. B: Environ*., **62**, 336 (2006).
35. S. Suárez, S. M. Jung, P. Avila, P. Grange and J. Blanco, *Catal. Today*, **75**, 331 (2002).
36. N. Bogdanchikova, F. C. Meunier, M. Avalos-Borja, J. P. Breen and A. Pestryakov, *Appl. Catal. B: Environ*., **36**, 287 (2002).
37. E. Kikuchi and K. Yogo, *Catal. Today*, **22**, 73 (1994).
38. R. Brosius, D. Habermacher, J. A. Martens, L. Vradman, M. Herskowitz, L. Čapek, Z. Sobalík, J. Dědeček, B. Wichterlová, Tokarová and O. Gonsiorová, *Topics Catal*., **30-31**, 333 (2004).
39. L. Čapek, L. Vradman, P. Sazama, M. Herskowitz, B. Wicherlov, R. Zukerman, R. Brosius and J. A. Martens, *Appl. Catal. B: Environ*., **70**, 53 (2007).
40. J. Y. Yan, H. H. Kung, W. M. H. Sachtler and M. C. Kung, *J. Catal*., **175**, 294 (1998).
41. G. Bagnasco, M. Turco, C. Resini, T. Montanari, M. Bevilacqua and G. Busca, *J. Catal*., **225**, 536 (2004).
42. C. Resini, T. Montanari, L. Nappi, G. Bagnasco, M. Turco, G. Busca, F. Bregani, M. Notaro and G. Rocchini, *J. Catal*., **214**, 179 (2003).
43. M. M. Yung, E. M. Holmgreen and U. S. Ozkan, *J. Catal*., **247**, 356 (2007).
44. Q. Wang, S. Y. Park, J. S. Choi and J. S. Chung, *Appl. Catal. B: Environ*., **79**, 101 (2008).
45. Q. Wang, S. Y. Park, L. Duan and J. S. Chung, *Appl. Catal. B: Environ.*, **85**, 10 (2008).
46. M. F. Irfan, J. H. Goo and S. D. Kim, *Appl. Catal. B: Environ*., **78**, 267 (2008).
47. G. Bergeret and P. Gallezot, in *Handbook of heterogeneous catalysis*, G. Ertl, H. Knozinger and J. Weitkamp Eds., VCH, New York, 446-450 (1997).